

Evaluation of the Bending Properties of Modified Fast-growing Poplar Glulam Based on Composite Mechanics

Zhenhua Han,^{a,*} Ray Zhang,^b and Boqi Song^a

Currently, the bending properties of glulam made from fast-growing poplar barely meet the requirements for application. In this study, the bending properties of glulam made from preservative alkaline copper quaternary (ACQ)-treated and phenol-formaldehyde resin reinforced poplar in different laminate configurations were full-scale tested via a four-point bending method. Theoretical models including stiffness model and rigidity model under different loading modes were founded based on the mechanical analysis of composite materials to predict the Young's modulus of bending and bending strength. The Young's modulus and bending strength of modified fast-growing poplar glulam was greatly enhanced compared with untreated ones, which can meet the standard requirements for symmetrical mixed-grade composition glulam grade E85-F255. The Young's modulus was predicted with the rigidity model with high accuracy. The relative error was below 12%. The modified stiffness model with correction factors for normal stress and interlayer tension shearing stress can also accurately predict the failure mode and bending strength.

Keywords: Glulam; Modified fast-growing poplar; Mechanical model; Bending properties; Shear strength

Contact information: a: Engineering General Institute of Shanghai Construction Group, Shanghai 201114, China; b: Salice China (Shanghai) Co. Ltd., Shanghai 201702, China);

* Corresponding author: hanzhenhua_520@126.com

INTRODUCTION

Glulam is widely used as an important component in modern timber structures as beams, columns, and other supporting members. It is laminated with wood laminae in the grain parallel direction and bonded together with adhesive in thickness, width, and length. Because the glulam is as cost-effective as a wood resource, freely designed, safe, and dimensionally stable, it is one of the most economical approaches for utilization of small-size wood pieces.

Poplar is one of the most important fast-growing species in China. It is widespread, well-adapted for various climates, and has a short growth cycle of almost 10 years. However, poplar wood is loose in structure, soft, rots easily, and has low strength, such that it can hardly meet the requirements of structural components (Herawati *et al.* 2010). Many research studies on wood reinforcement have been carried out to overcome the low-strength shortage of fast-growing poplar wood for glulam members. Mirzaei *et al.* (2017) found that the moisture induced stress of glulam beams made from hydrothermally treated poplar was reduced and the bending strength was increased. Besides, the wood cell lumen, as well as cell walls can be strengthened after fiber reinforced polymer (FRP) treatment, which efficiently improves the strength of modified

glulam (Yang and Liu 2007; Cheng and Hu 2011; Osmannezhad *et al.* 2014). Wood as a kind of biomass material easily decays, rots, or degrades, which may largely shorten the life cycle of timber structures. It is important to carry out some durability treatments to ensure the safety for designed service life. Herzog *et al.* (2004) and Yang *et al.* (2012) have studied the influence of preservative treatments on wood mechanical properties. The results show that the excess ethanolamine in preservatives can partly depolymerize the lignin and decrease the MOE (Herzog *et al.* 2004; Gaspar *et al.* 2009; Yang *et al.* 2012). However, due to the variability of wooden materials, the mechanical properties of glulam made from modified wood can hardly be evaluated accurately.

Glulam made from fast-growing modified poplar is a laminated structure, and its mechanical strength varies with lamina types and configuration. Falk and Colling (1995) have investigated the influence of different configuration plans to optimize the laminae configuration. The glulam shows better bending properties when the higher-grade laminae are positioned in the member where the service load is expected to create higher stress. Conversely, lower-grade laminations are positioned in the areas where the stress is expected to be lower (Falk and Colling 1995). Yang used a strain gauge method to explore the strain and stress of laminae during bending and determined the effect of laminate configuration on the MOE of glulam (Yang *et al.* 2007). However, the research was based on the experimental data of single laminae strength. The bonding strength between layers can also affect the bending properties of glulam.

In order to determine the mechanical properties of glulam and apply them in the structure, it is common practice to prepare numerous destructive full-scale experiments. However, such an approach can be both ineffective and wasteful. It is indispensable to build a model for modified fast-growing poplar glulam strength and figure out the strength of any configuration. In this research, the bending properties of glulam were theoretically investigated based on the mechanical analysis of composite materials. Full-scale tests were carried out on the glulam made from reinforced or preservative modified poplar wood to verify the model.

EXPERIMENTAL

Wood Members

The experimental groups were named as follows. A is the control group, untreated fast-growing poplar (*Populus tomentosa* Carr.) with a density of 0.38 g/cm³ and moisture content of 12%. B is the preservative ACQ modified fast-growing poplar. C is the phenol formaldehyde resin (PF) reinforced fast-growing poplar. D represents the preservative ACQ together with PF modified fast-growing poplar.

The bending strength, Young's modulus, compressive, and tensile strength, along the grain of the wood member specimen were tested according to GB/T 1936.1 (2009), GB/T 1936.2 (2009), GB/T 1935 (2009), and GB/T 1938 (2009). Five parallel experiments were conducted for each type of sample to get the average mechanical properties.

Two of same wood members and two different members were glued together with single-component polyurethane resin and the bonding strength were tested according to GB/T 26899 (2011). The single spreading ratio was 200 g/m². Each group contained three samples to get the average bonding strength.

Manufacture of Glulam

Different kinds of wood elements were assigned to assemble the 5-ply glulam. The pre-laminations were initially trimmed by a finger-joint machine at both ends. Then they were matched and mounted by using the single-component polyurethane resin under a pressure of 0.5 MPa for 24 h and then planed to 20 mm thick. The actual thickness of each lamina is illustrated in Table 1. The single-component polyurethane resin was utilized as an adhesive at the single spread ratio of 200 g/m². The strips were quickly assembled together after glue spreading. Then they were clamped tightly at room temperature for 24 h until curing. The glulam dimensions were 1.95 m in length, 45 mm in width, and approximately 20 mm in thickness. The laminate configuration and thickness for each layer are shown in Table 1.

Table 1. Laminate Configuration of Glulam Beams

No.	Length <i>L</i> (m)	Width <i>b</i> (mm)	Thickness of Each Lamina (mm)				
			A	A	A	A	A
0	1.95	45	20.2	20.2	20.2	20.2	20.2
1	1.95	45	20.3	20.3	20.3	20.3	20.3
2	1.95	45	20.2	20.2	20.2	20.2	20.2
3	1.95	45	23	20	26	20	23
4	1.95	45	20.2	20.2	20.2	20.2	20.2
5	1.95	45	20.5	20.5	25	20.5	20.5

Bending Tests of Glulam

As shown in Fig. 1, the bending strength and Young's modulus of glulam were tested with four-point bending method. The tests were carried out in accordance with GB/T 26899-2011, Structural glued laminated timber Bending test A, on the mechanical testing machine (WDW-200E, Jinan TimeShiJin Instruments Co. Ltd, Jinan, China). The load was applied at a speed rate of 14.7 MPa/min. Each glulam group contains 3 parallel samples. The Young's modulus *E* (MOE) was calculated by Eq. 1,

$$E = \frac{P}{\omega} \cdot \frac{23L^3}{108bh^3} = \frac{\Delta P}{\Delta \omega} \cdot \frac{23L^3}{108bh^3} = k \cdot \frac{23L^3}{108bh^3} \quad (1)$$

where *P* is loading strength on the glulam beam, *ω* is the deflection at middle point, *L* is the span of the beam, *b* is the width, *h* is the height of the beam, and *k* = ($\Delta P/\Delta \omega$) represents the linear gradient of loading-deflection curve. The bending strength MOR σ_b

of glulam can be calculated by Eq. 2.

$$\sigma_b = \frac{PL}{bh^2} \quad (2)$$



Fig. 1. Four-point bending test of glulam

THEORETICAL MODELS

Stiffness Model

According to the mechanics of the composite material constitutive principle, the glulam can be equivalent to synthetic laminated structures and with no coupling effect between layers. The stiffness of glulam was represented by Young's modulus in practice. As the bending member in the structure, the Young's modulus in the direction of x-axis was analyzed in this study.

Figure 2 illustrates the mechanical analysis of glulam subjected to bending. The adhesive layer between wood laminae can be ignored because it can be so thin. The mechanical properties of glulam in vertical directions is content with parallel models. As the lateral shearing stress on each layer and transverse plane are different when bending, the strain of each layer is complex to describe. In this way, the Young's modulus of composite beams in the direction of x-axis can be obtained from Eq. 3 (Zhang *et al.* 1992),

$$E_L = \frac{\overline{EI}}{I_y} \quad (3)$$

where I_y is the inertia moment to neutral axis y at the cross section, and \overline{EI} is the flexural stiffness to neutral axis y at the cross section, which can also be represented by Eq. 4, where n is number of layers, k represents the k_{th} layer, z is the distance to the neutral axis y .

$$\overline{EI} = \int_A E_x^{(k)} z^2 dA = \sum_{k=1}^n E_x^{(k)} I_y^{(k)} \tag{4}$$

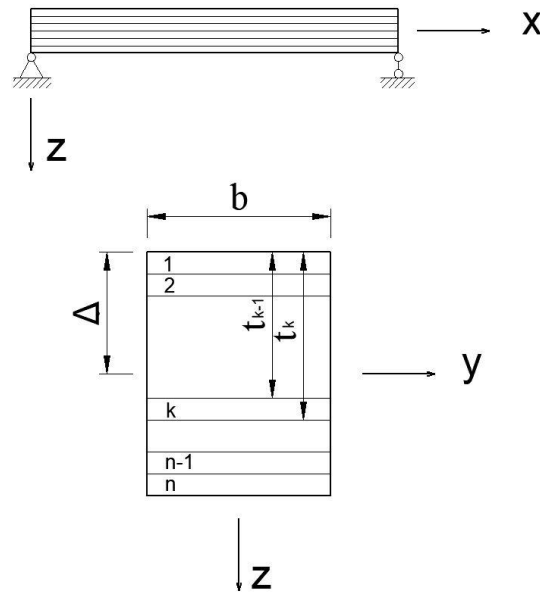


Fig. 2. Mechanical analysis of glulam

As for symmetrical laminated structure and unsymmetrical laminated structure, \overline{EI} is calculated by Eq. 5,

$$\overline{EI} = E_x^f I_y = \frac{b}{d_{11}} = \frac{b}{3} \sum_{k=1}^n E_x^{(k)} \left[(t_k^3 - t_{k-1}^3) - 3\Delta^2 (t_k - t_{k-1}) \right] \tag{5}$$

where $I_y^{(k)}$ is the inertia moment of the k^{th} layer on the neutral axis y , b is the width of the layer, t_k is the distance of the k^{th} layer bottom plane to the upper plane of glulam, d_{11} is the flexural coefficient of symmetrical structure, $E_x^{(k)}$ is the Young's modulus of the k^{th} layer in x direction, and Δ represents the distance of the neutral axis y to glulam upper plane, which can be calculated by Eq. 6:

$$\Delta = \frac{1 \sum_{k=1}^n E_x^{(k)} (t_k^2 - t_{k-1}^2)}{2 \sum_{k=1}^n E_x^{(k)} (t_k - t_{k-1})} \tag{6}$$

Rigidity Model

The glulam mainly supports the bending moment in the thickness direction in the timber structure. It can be derived from stress and experience analysis that the two main failure modes are normal stress failure in which the layer strips are snapped or crushed under normal stress, and shearing failure between layers, which means that the glue line is damaged under the shearing load. In this study, these two failure modes are discussed respectively.

As for normal stress failure, the normal stress of every layer at a cross section is analyzed separately. The normal stress of a single layer σ_x can be represented by Eq. 7,

$$\sigma_x = \frac{ME_x^{(k)}z}{EI} \quad (7)$$

where M is the bending moment at cross section. To keep the glulam from failure, the normal stress of any layer should meet the demand as follows,

$$|\sigma_x| \leq [\sigma_i] \quad (8)$$

where $[\sigma_i]$ is allowable stress of a single layer. When $\sigma_x > 0$, $[\sigma_i]$ is allowable tension stress. When $\sigma_x < 0$, $[\sigma_i]$ is allowable compression stress.

As for the shearing failure between layers, the shearing stress of every glue line is analyzed separately. The shearing stress of a single layer τ_k can be obtained by Eq. 9,

$$\tau_k = \frac{Q \sum_{i=k}^n E_x^{(i)} S_i}{E I b} \quad (9)$$

where S_i is the static moment of the i^{th} layer area that from z_k to z_n on neutral axis y , and τ_k is the shearing stress between the k^{th} layer and the $(k+1)^{\text{th}}$ layer.

To keep the glulam from failure, the shearing stress between each two layers should meet that:

$$\tau_k \leq q_i \quad (10)$$

where q_i is the bonding strength between layers.

It can be derived from Eqs. 7 and 8 that the bending moment M induced by normal stress should meet Eq. 11, and the shearing stress Q that caused shearing stress between layers should meet Eq. 12.

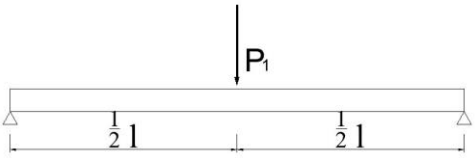
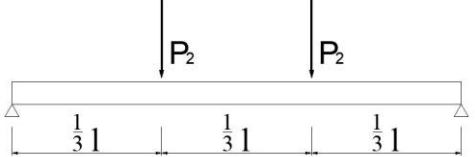
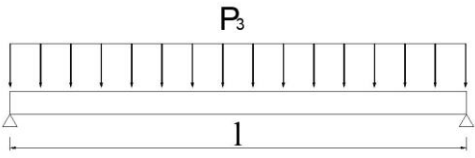
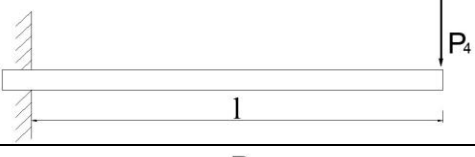
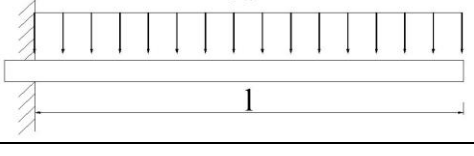
$$M \leq \frac{EI[\sigma_i]}{E_x^{(k)}z} \quad (11)$$

$$Q \leq \frac{E I b q_i}{\sum_{i=k}^n E_x^{(i)} S_i} \quad (12)$$

Loading Mode

The bending strength of glulam is the combination of Eqs. 11 and 12. As shown in Table 2, the maximum bending moment M_{max} , the maximum shearing stress Q_{max} and their corresponding relationship can be defined when the loading mode on glulam is definite. (Chen and Yang 2006). In this way, the maximum bending moment for glulam can be derived from Eqs. 11, 12, and Table 2.

Table 2. The Bending Moment and Shearing Stress of Glulam vs. Loading Mode

Support and Loading	Q_{max}	M_{max}	Corresponding relationship	Illustration
supported on both sides and the loading P_1 concentrates at the middle point	$\frac{P_1}{2}$	$\frac{P_1 l}{4}$	$M_{max} = Q_{max} \frac{l}{2}$	
supported on both sides and the loading P_2 concentrates at each of the two trisection points	$\frac{P_2}{2}$	$\frac{P_2 l}{6}$	$M_{max} = Q_{max} \frac{l}{3}$	
supported on both sides and the loading P_3 is uniformly distributed on the beam	$\frac{P_3 l}{2}$	$\frac{P_3 l^2}{8}$	$M_{max} = Q_{max} \frac{l}{4}$	
loading P_4 concentrates at the free end of the cantilever beam	P_4	$P_4 l$	$M_{max} = Q_{max} l$	
the cantilever beam is uniformly loaded	$P_3 l$	$\frac{P_3 l^2}{2}$	$M_{max} = Q_{max} \frac{l}{2}$	

$$M_{max} = \begin{cases} \text{Min} \left(\frac{\overline{EI}[\sigma_i]}{E_x^{(k)} z}, \frac{l \overline{EI} b q_i}{2 \sum_{k=1}^n E_x^{(i)} S_i} \right) & \text{Loading at the middle point of simple supported beam} \\ & \text{or uniform loading on cantilever beam} \\ \\ \text{Min} \left(\frac{\overline{EI}[\sigma_i]}{E_x^{(k)} z}, \frac{l \overline{EI} b q_i}{3 \sum_{k=1}^n E_x^{(i)} S_i} \right) & \text{Loading at the trisection points of simple supported beam} \\ \\ \text{Min} \left(\frac{\overline{EI}[\sigma_i]}{E_x^{(k)} z}, \frac{l \overline{EI} b q_i}{4 \sum_{k=1}^n E_x^{(i)} S_i} \right) & \text{Uniform loading on simple supported beam} \\ \\ \text{Min} \left(\frac{\overline{EI}[\sigma_i]}{E_x^{(k)} z}, \frac{l \overline{EI} b q_i}{\sum_{k=1}^n E_x^{(i)} S_i} \right) & \text{Loading at the free end of cantilever beam} \end{cases} \tag{13}$$

The MOR of the rectangular cross section beam is shown in Eq. 14:

$$\sigma_b = \frac{M}{W} = \frac{6M}{bh^2} \tag{14}$$

The rigidity model of glulam can be derived as follows.

$$\sigma_b = \left\{ \begin{array}{l} \text{Min} \left(\frac{6\overline{EI}[\sigma_i]}{bh^2 E_x^{(k)} z}, \frac{3\overline{EI}bq_i}{bh^2 \sum_{k=1}^n E_x^{(i)} S_i} \right) \quad \begin{array}{l} \text{Loading at the middle point of simple supported beam} \\ \text{or uniform loading on cantilever beam} \end{array} \\ \text{Min} \left(\frac{6\overline{EI}[\sigma_i]}{bh^2 E_x^{(k)} z}, \frac{2\overline{EI}bq_i}{bh^2 \sum_{k=1}^n E_x^{(i)} S_i} \right) \quad \text{Loading at the trisection points of simple supported beam} \\ \text{Min} \left(\frac{6\overline{EI}[\sigma_i]}{bh^2 E_x^{(k)} z}, \frac{3\overline{EI}bq_i}{2bh^2 \sum_{k=1}^n E_x^{(i)} S_i} \right) \quad \text{Uniform loading on simple supported beam} \\ \text{Min} \left(\frac{6\overline{EI}[\sigma_i]}{bh^2 E_x^{(k)} z}, \frac{6\overline{EI}bq_i}{bh^2 \sum_{k=1}^n E_x^{(i)} S_i} \right) \quad \text{Loading at the free end of cantilever beam} \end{array} \right. \tag{15}$$

RESULTS AND DISCUSSION

Mechanical Properties of Wood Members

The mechanical properties of different wood members and bonding strength between each two members are shown in Tables 3 and 4. The mechanical properties of fast-growing poplar wood were improved slightly after preservative treatment, which is in opposition with the previous research conclusions (Yang *et al.* 2012). This may result from short modification time and different preservative solvents. The bending properties of PF reinforced poplar wood were larger than those of the untreated group.

Table 3. Mechanical Properties of Wood Members*

Sample	Bending Strength (MPa)	Young's Modulus (MPa)	Compressive Strength (MPa)	Tensile Strength (MPa)
A	71.12(5.6)	5493.35(14.4)	55.34(18.0)	100.81(10.7)
B	82.35(21.5)	8159.15(20.9)	84.42(19.2)	110.82(23.6)
C	105.61(12.8)	9428.15(11.9)	103.21(29.3)	138.12(24.2)
D	108.34(15.0)	9360.48(18.5)	106.55(36.0)	133.67(38.1)

* Values in parentheses are coefficients of variation in percent.

Table 4. Bonding Strength of Single-Component Poly-Urethane Resin Adhesive Samples (MPa)

	A	B	C	D
A	11.92(19.8)	12.57(16.9)	13.73(24.8)	11.38(15.1)
B		12.63(28.1)	11.56(10.9)	15.90(39.5)
C			11.91(76.1)	12.30(24.8)
D				14.93(39.7)

The preservative modification had little impact on the PF reinforced wood, while there was no obvious relationship between the bonding strength of untreated groups and that of modified groups.

Model Validation

The glulam bending average test results and model calculated results of MOE and MOR are illustrated in Table 5. The MOE and MOR of glulam made from untreated fast-growing poplar wood can hardly meet the Japanese standard JAS 1152 (2007) Glued laminated timber for symmetrical mixed-grade composition glulam. However, the mechanical properties were greatly enhanced after preservative treatments and reinforcement modification. Taking the size of common glulam beams that the size effect should be noticed on the test results. According to Zhou's research, the size impact on MOE is not significant (Zhou *et al.* 2016). While the bending strength of the timber as well as glulam follows the Weibull distribution, which is also called the weakest link theory (Weibull 1939). This theory suggests that the strength of the component is determined by the weakest zone.

Table 5. Test and Calculation Results of MOE and MOR

No.	h (mm)	P_{max} (kN)	MOE(MPa)			MOR(MPa)		
			Actual value	Prediction value	Relative error(%)	Actual value	Prediction value	Relative error(%)
0	101	11.1(10.2)	5245.15(34.1)	5493.35	4.73	43.53(26.7)•	55.34•	27.14
1	101	16.7(21.0)	8449.03(29.4)	8138.32	3.68	65.48(23.1)•	84.20•	28.58
2	101	19(8.9)	8917.82(16.7)	9132.82	2.41	74.50(19.1)•	99.98•	34.2
3	112	21.5(26.7)	9121.24(30.8)	9081.37	0.44	68.56(45.5)▲	103.37•	50.78
4*	101	16(26.0)	7961.48(48.6)	7028.23	11.72	62.74(14.8)•	110.24•	75.71
5	107	15.8(30.4)	9428.73(58.2)	9078.67	3.71	55.20(20.4)▲	103.34•	87.21

* In sample 4#, the wood failure between layer strips C and D was below 60% and the PF resin was not cured completed. MOE of strip C 7973.83MPa and strip D 6793.02MPa were used in the calculation.

• normal stress failure, ▲ shearing failure between layers

With the size getting larger, more defects and it is more probably to get failure. Bohannan (1966) thought that the bending strength was not affected by the width of specimen but span-to-depth ratio, which is often constant in structural component. So the bending strength of the glulam beam with span 2600 mm can be transformed with Eq. 16,

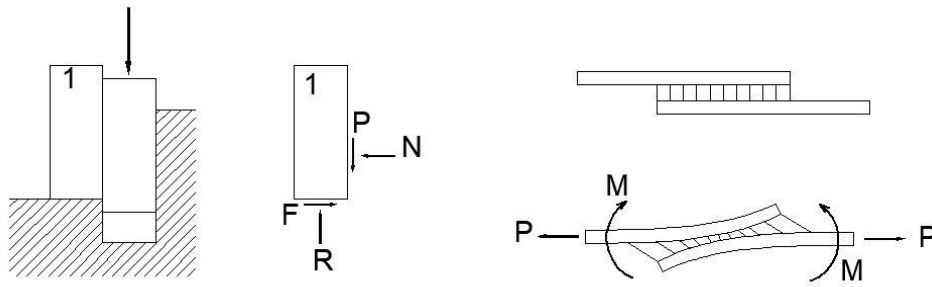
$$\frac{\sigma_1}{\sigma_2} = \left(\frac{L_2}{L_1} \right)^{k_{hl}} \quad (16)$$

where σ_1 and L_1 are the bending strength and span of the test specimen, σ_2 and L_2 are the bending strength and span of the common-size glulam beam, and k_{hl} is the composite size effect coefficient of length and height. According to Zhou's size effect coefficient research results of $k_{hl} = 0.275$, the calculated bending strength of glulam beam with span 2600 mm for configuration 5 is 51.0 MPa, which meet the JAS standard strength grade for E85-F255. Hence the modified glulam beams are qualified for utilization.

Table 5 shows that the glulam MOE test values approximately agreed with the prediction values, and the relative errors were below 12%. In other words, the stiffness properties of glulam can be simulated using theoretical models and the mechanical strength of wood members. The MOE of glulam is supposed to decline when produced from small wood members. In this way, the test values were supposed to be smaller than prediction values. However, there was no certain relationship between actual values and prediction values. It is probably because wood is asymmetrical in structure, and the variability was enhanced after impregnating modification. As a result, the scale effect was concealed. And the deviations between the test results and prediction values were relatively small. In this way, the glulam stiffness model was accurate in prediction. However, the predictive shearing strength values between layers were higher than actual values. The model can hardly predict the shearing failure between layers and the deviation was relatively high. This is probably because of the offset of bonding test results.

Model Adjustment

As shown in Fig. 3(a), the bonding strength between layers was tested in a compression shear method. It can be derived from mechanical analysis for block 1 that the upward supporting force balanced the downward compression force P in the vertical direction. However, the supporting force R cannot entirely apply to the glue line and it was on a different vertical plane with compression force P . Thus, there was a moment induced from R and P . In order to balance the moment, there must have been a compression stress N to the left direction on the glue line of block 1. Meanwhile, there was friction F between clamps and the bottom of block 1 to balance the leftward compression stress N . The moment induced from friction F and compression stress N was equal to the moments induced from upward supporting force R and downward compression force P . Figure 3(b) shows the bonding strength test in tension mode. As the sample was not limited by clamps and the tension shearing stress of the test sample was not on the same plane when applying tension loading P on both sides, there were two equal moments M on both blocks that induced both shearing stress and normal stress. The normal stress performed as compression loading in the middle of the shearing area, and it performed as increasing tension loading at both ends of the shearing area.



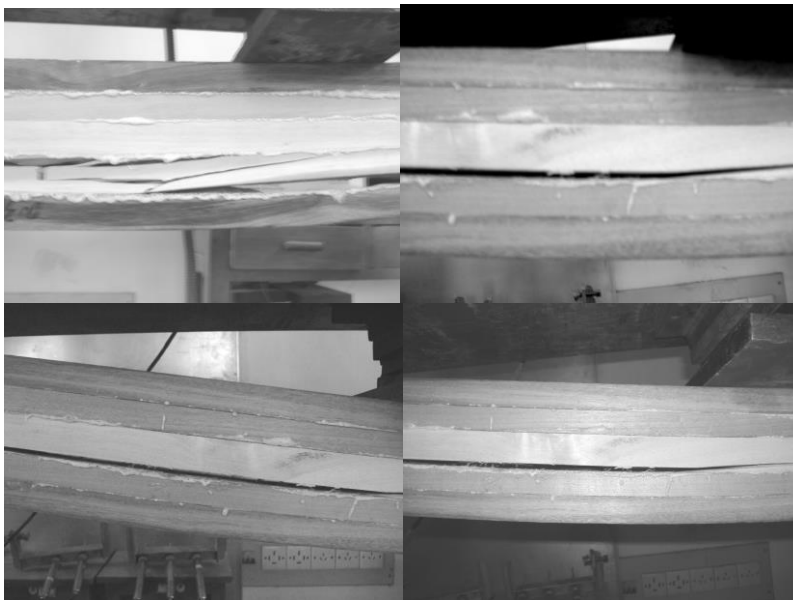
(a) compression shear

(b) tension shear

Fig. 3. Test methods of two different shear strength

Therefore, the strength in the shearing area was not only shearing stress but also considerable normal stress in the shearing area when testing in compression shear methods. The normal stress was also concentrated and with the same magnitude as the shearing stress. The normal stress was manifested as a compression stress that prevented the damage of adhesive wood elements when the loading was in compressing directions. However, when the loading was in tension direction, the normal stress performed as tension stress that promoted the observed failure.

However, there was not only shearing stress but also normal stress between layers in glulam bending according to the three-dimensional stress analysis theory. The normal stress at the tension layer near the ends performed as tension stress that promoted the failure between layers. The normal stress at the compression layer near the ends performed as compression stress that prevented the damage. In other words, the weakest interlayer sections were located in the tension layer of the ends. As shown in Fig. 4, the interlayer failure mode in the tests was also consistent with the prediction.

**Fig. 4.** Shearing failure between layers in glulam

In short, the interlayer shearing failure of glulam was a result from tension and shearing effects. This failure mode was much closer to the bonding test in tension shearing methods. The bonding strength between layers were tested in compression and tension shearing methods and the results are shown in Table 6.

Table 6. Bonding Strength under Tension Shear Method (MPa)

	A	B	C	D
A	3.32(10.9)	3.56(34.1)	3.36(8.4)	3.21(17.9)
B		2.55(21.8)	2.53(14.6)	2.59(20.6)
C			2.79(11.3)	3.04(13.1)
D				3.41(30.7)

A comparison between Tables 4 and 6 shows that the tension shear strength was about 1/3 of the compression shear strength. The interlayer normal stress had great influence on the shearing strength between layers. In order to get more accurate simulation results, the tension shear strengths were re-assigned in the model, and the normal stress and interlayer shearing strength were modified with coefficients. In the modified model, the normal stress was multiplied by correction factor k_1 for the deviation of layer strips and negative effects of defections, $k_1=0.8$. The interlayer shearing stress was multiplied by correction factor k_2 to represent the strength loss from poor adhesives, as the glue layer can soften the strength decline from strip defection to some extent, $k_2=0.9$. The results are shown in Table 6.

Table 7 shows that the modified model was able to predict the failure mode and bending strength within a small error range after re-assignment with tension shear stress and correction factors. The model prediction coincides the actual failure mode except for glulam #4, which was probably because the resin between the layers did not completely solidify which resulted in the decrease of the shearing strength.

Table 7. MOR Results Calculated with Modified Model

No.	h (mm)	P_{max} (kN)	Actual value	Re-assignment with tension shear strength		Model modified with coefficients	
				Prediction value	Relative error(%)	Prediction value	Relative error(%)
0	101	11.1(10.2)	43.53(26.7)•	55.34•	27.14	44.27•	1.71
1	101	16.7(21.0)	65.48(23.1)•	84.20•	28.58	67.36•	2.87
2	101	19(8.9)	74.50(19.1)•	88.86•	19.27	79.98•	7.35
3	112	21.5(26.7)	68.56(45.5)▲	81.01▲	18.16	73.32▲	6.94
4	101	16(26.0)	62.74(14.8)•	82.82▲	32.01	79.91▲	27.37
5	107	15.8(30.4)	55.20(20.4)▲	61.39▲	11.21	55.25▲	0.09

It must be noted that the evaluation of the normal stress correction factor k_1 and interlayer shearing stress correction factor k_2 were significant in glulam strength prediction. As the strength loss of normal stress and interlayer shearing stress varies in different situations, they should be evaluated according to the sample actual conditions.

CONCLUSIONS

1. The Young's modulus and bending strength of modified fast-growing poplar wood members and glulam were greatly enhanced compared with those of untreated groups. While the bonding strength before and after modification changed little. The reinforced modification can strengthen the glulam, and the mechanical properties met the JAS standard requirement for symmetrical mixed-grade composition glulam grade E85-F255.
2. The Young's modulus of glulam can be predicted by the rigidity model with high accuracy. The relative error was below 12%, while the deviation between glulam stiffness model prediction values and test results was higher because the interlayer shearing strength tested in compression shearing method is largely affected by normal stress. It can be derived from stress analysis and experiments that the tension shear strength is about 1/3 of the compression shear strength.
3. The modified model was able to accurately predict the failure mode and bending strength with correction factors for normal stress and interlayer tension shearing stress. The deviation was also diminished to an allowable range. It can be used to guide the optimization design of glulam mix-grade laminate configurations.

ACKNOWLEDGEMENTS

The authors gratefully acknowledge the financial support from Research Program supported by Housing and urban-rural development "Application analysis of timber structure in new architecture industrialization practice based on different structural materials and system" (2016-K5-003) and the research project supported by Shanghai Construction Group "Research on the CLT structural system and key technology of prefabrication" (15JCYJ-02).

REFERENCES CITED

- Bohannon, B. (1966). "Effect of size on bending strength of wood members," US Forest Service Research Paper FPL, 56.
- Chen, L. M., and Yang, B. N. (2006). *Mechanic Analysis of Composite Material [in Chinese]*, China Science Press, Beijing, China.
- Cheng, F., and Hu, Y. (2011). "Nondestructive test and prediction of MOE of FRP reinforced fast-growing poplar glulam," *Composites Science & Technology* 71, 1163-1170.

- Falk, R. H., and Colling, F. (1995). "Laminating effects in glued-laminated timber beams," *Journal of Structural Engineering* 121, 1857-1863. DOI: 10.1061/(ASCE)0733-9445(1995)121:12(1857)
- Gaspar, F., Cruz, H., Gomes, A., and Nunes, L. (2009). "Production of glued laminated timber with copper azole treated maritime pine," *European Journal of Wood & Wood Products* 68(2), 207-218. DOI: 10.1007/s00107-009-0373-6
- GB/T 1936.1 (2009). "Method of testing in bending strength of wood," Standardization Administration of China, Beijing, China.
- GB/T 1936.2 (2009). "Method for determination of modulus of elasticity in static bending of wood," Standardization Administration of China, Beijing, China.
- GB/T 1935 (2009). "Method of testing compressive strength parallel to grain of wood," Standardization Administration of China, Beijing, China.
- GB/T 1938 (2009). "Method of testing tensile strength parallel to grain of wood," Standardization Administration of China, Beijing, China.
- GB/T 26899(2011). "Structural glued laminated timber," Standardization Administration of China, Beijing, China.
- Herawati, E., Massijaya, M. Y., and Nugroho, N. (2010). "Performance of glued-laminated beams made from small diameter fast-growing tree species," *Journal of Biological Sciences* 10, 37-42. DOI: 10.3923/jbs.2010.37.42
- Herzog, B., Goodell, B., Lopez-Anido, R., Muszynski, L., Gardner, D. J., Halteman, W. and Qian, Y. (2004). "The effect of creosote and copper naphthenate preservative systems on the adhesive bondlines of FRP/glulam composite beams," *Forest Products Journal* 54, 82-90.
- JAS 1152 (2007). "Japanese agricultural standard for glued laminated timber," Ministry of 383 Agriculture, Forestry, and Fisheries, Tokyo, Japan.
- Mirzaei, G., Mohebbi, B., and Ebrahimi, G. (2017). "Glulam beam made from hydrothermally treated poplar wood with reduced moisture induced stresses," *Construction & Building Materials* 135, 386-393. DOI: 10.1016/j.conbuildmat.2016.12.178
- Osmannezhad, S., Faezipour, M., and Ebrahimi, G. (2014). "Effects of GFRP on bending strength of glulam made of poplar (*Populus deltoids*) and beech (*Fagus orientalis*)," *Construction & Building Materials* 51, 34-39. DOI: 10.1016/j.conbuildmat.2013.10.035
- Weibull, W. (1939). "A statistical theory of the strength of materials," *Proceedings of the American Mathematical Society* 151(5), 1034-1034.
- Yang, H., and Liu, W. (2007). "Study on flexural behavior of FRP reinforced glulam beams," *Journal of Building Structures* 28(1), 64-71.
- Yang, T. H., Lin, C. H., Wang, S. Y., and Lin, F. C. (2012). "Effects of ACQ preservative treatment on the mechanical properties of hardwood glulam," *European Journal of Wood & Wood Products* 70(5), 557-564.
- Yang, T. H., Wang, S. Y., Lin, C. J., Tsai, M. J., and Lin, F. C. (2007). "Effect of laminate configuration on the modulus of elasticity of glulam evaluated using a strain gauge method," *Journal of Wood Science* 53(1), 31-39.

Zhang, S. Y., Liu,, J. Q., Yu X. X., and Cai, L. W. (1992). *Mechanical Properties of Composite Structure, [in Chinese]*, Beijing Institute of Technology Press, Beijing, China.

Zhou, X. Y., Cao, L., and Zeng, D. (2016). “Experimental study on the size effect on flexural behavior of larch glulam beams,” *Applied Mechanics & Materials* 847, 3-9.

Article submitted: February 13, 2018; Peer review completed: May 24, 2018; Revised version received: July 10, 2018; Accepted: July 11, 2018; Published: August 1, 2018.
DOI: 10.15376/biores.13.3.7071-7085